Regulation of Exocytotic Fusion by Cell Inflation

Carles Solsona,* Barbara Innocenti,# and Julio M. Fernández§

§Department of Physiology and Biophysics, Mayo Foundation, Rochester, Minnesota 55905 USA; *Molecular and Cellular Neurobiology, Department of Cell Biology, Medical School, University of Barcelona, Barcelona, Spain; and #Department of Biomedical Sciences, University of Padua, Padua, Italy

ABSTRACT We have inflated patch-clamped mast cells by 3.8 ± 1.6 times their volume by applying a hydrostatic pressure of 5–15 cm H_2O to the interior of the patch pipette. Inflation did not cause changes in the cell membrane conductance and caused only a small reversible change in the cell membrane capacitance (36 ± 5 fF/cm H_2O). The specific cell membrane capacitance of inflated cells was found to be 0.5 $\mu F/cm^2$. High-resolution capacitance recordings showed that inflation reduced the frequency of exocytotic fusion events by ~70-fold, with the remaining fusion events showing an unusual time course. Shortly after the pressure was returned to 0 cm H_2O, mast cells regained their normal size and appearance and degranulated completely, even after remaining inflated for up to 60 min. We interpret these observations as an indication that inflated mast cells reversibly disassemble the structures that regulate exocytotic fusion. Upon returning to its normal size, the cell cytosol reassembles the fusion pore scaffolds and allows exocytosis to proceed, suggesting that exocytotic fusion does not require soluble proteins. Reassembly of the fusion pore can be prevented by inflating the cells with solutions containing the protease pronase, which completely blocked exocytosis. We also interpret these results as evidence that the activity of the fusion pore is sensitive to the tension of the plasma membrane.

INTRODUCTION

Synaptic transmission is carried out in nerve terminals by exocytosis of synaptic vesicles. The small size of nerve terminals and synaptic vesicles makes it difficult to gain direct access to measure the events that lead to vesicle fusion. However, it is generally thought that the basic mechanisms of exocytosis are conserved. Because of their spherical shape and secretory granule size, mast cells are suitable for the study of the basic mechanisms of exocytosis. The plasma membrane plays a crucial role in exocytosis. In electron micrographs of mast cells, the first event observed in response to a secretory stimulus is dimpling of the plasma membrane toward the membrane of adjacent secretory granules (Chandler and Heuser, 1980). It has been suggested that the plasma membrane dimple is caused by a scaffold of proteins, which is represented as a series of filaments constituting a polymeric structural molecule, along which are arranged regulatory and effector molecules (Monck and Fernandez, 1994). Upon activation, the plasma membrane is drawn into the scaffold center. The tip of the resulting dimple becomes highly curved, and it is thought that it spontaneously fuses with the vesicle membrane, resulting in hemifusion (Monck and Fernandez, 1994; Kemble et al., 1994). In this model, breakup of the hemifusion membrane creates a lipidic fusion pore that may close again during a transient fusion or expand irreversibly. Throughout these events the vesicle membrane is under tension, causing a large flux of lipids through the fusion pore and into the granule membrane (Monck et al., 1990). This view of exocytosis predicts that the formation of a fusion pore will be dependent on the physical parameters of the fusing membranes. For example, fusion pore formation causes sharp bending of the fusing membranes. Hence the size and kinetics of the fusion pore will be dependent on the spontaneous curvature of the fusing membranes and membrane tension (Nanavati et al., 1992; Zimmerberg et al., 1993).

Recent experiments with laser tweezers have shown that the resting plasma membrane tension is small, ~0.1–0.001 mN/m, and it is regulated by the local cytoskeleton (Hochmuth et al., 1996). Furthermore, the resting tension is thought to play an important role in regulating the balance between exocytosis/endocytosis and other cellular functions (Dai and Sheetz, 1995; Hochmuth et al., 1996).

In this paper we inflate patch-clamped mast cells by applying a hydrostatic pressure of 10–15 cm H_2O to the interior of the patch pipette (Setoguchi et al., 1997; Du and Sorota, 1997; Matsuda et al., 1996). Upon inflation, mast cells increase their volume by up to seven times and their plasma membrane tension by up to ~5 mN/m. We found that inflation of mast cells inhibited exocytosis and revealed a peculiar mode of vesicular fusion, as measured by capacitance recordings. The cell inflation technique is useful in other ways as well. For example, cell inflation permits an accurate estimate of the total cell membrane area, which, when combined with measurements of the total cell membrane capacitance, yielded a specific capacitance of 0.5 $\mu F/cm^2$.

Another useful application results from perfusion of the cytosol by cell inflation. The introduction of solutes into intact cells is typically accomplished with patch pipettes. After establishing the whole-cell mode patch-clamp recording, a narrow, micrometer-sized opening connects the pipette interior with the cell cytosol. Through this opening, a

Received for publication 30 April 1997 and in final form 4 November 1997.

Address reprint requests to Dr. Julio M. Fernandez, Department of Physiology and Biophysics, Mayo Clinic and Foundation, 1-159 Medical Sciences Building, Rochester, MN 55905. Tel.: 507-284-0423; Fax: 507-284-0521; E-mail: fernandez.julio@mayo.edu.

0006-3495/98/02/1061/13 $2.00

diffusion exchange of solutes between the pipette and the cytosol occurs. Small solutes equilibrate in a few seconds. However, the introduction of high-molecular-weight solutes, like antibodies, recombinant proteins, and toxins, is slow and uncertain. As an example, we show the blocking effects of pronase introduced into mast cells by inflation.

MATERIALS AND METHODS

Preparation of cells

Mast cells were obtained by lavage of the peritoneal cavity of adult male c57BL/6J mice (Jackson Laboratories, Bar Harbor, ME). The lavage solution consisted of CO_2 independent medium (GIBCO, BRL) complemented with bovine serum albumin (BSA) (1 mg/ml). The lavage was centrifuged, and the cell pellet was resuspended in BSA-free CO_2 independent medium. The resulting suspension of cells were plated onto glass-bottomed culture chambers and stored at room temperature until used.

Chromaffin cells were prepared from bovine adrenal medulla by enzymatic digestion. Isolated cells were suspended in Dulbecco's modified Eagle's medium (DMEM) supplemented with 25 mM HEPES, 10% fetal calf serum, 8 μM 5-fluoro-2′-deoxyuridine, 50 μg/ml gentamycin, 10 μM cytosine arabinofuranoside, 2.5 μg/ml fungizone, 25U/ml penicillin, and 25 μg/ml streptomycin. Chromaffin cells were plated, at a density of 100,000–300,000 cells/ml, onto glass-bottomed culture chambers. Cells were cultured in an incubator at 37°C and 5% CO_2 for 1–5 days before use.

Chinese hamster ovary (CHO) (ATTC) cells were plated onto glass-bottomed culture chambers. The cells were cultured in an incubator at 37°C and 5% CO_2. The culture medium consisted of DMEM F-12 medium (Gibco) supplemented with 2 mM glutamine and 10% fetal calf serum.

Solutions

The mast cell external medium was a modified Ringer's solution containing (mM) 150 NaCl, 2.8 KOH, 10 HEPES, 1.5 NaOH, 1 $MgCl_2$, 2 $CaCl_2$, and 25 glucose (310 mmol/kg, pH 7.25). The chromaffin cell and CHO cell external medium was (mM) 140 NaCl, 10 HEPES, ~1.5 NaOH, 2 $MgCl_2$, 2 $CaCl_2$, and 25 glucose (310 mmol/kg, pH 7.25). We added 1 μM TTX to the external solution used for recordings in chromaffin cells.

The mast cell pipette recording solutions contained (in mM) 125 K-glutamate, 10 HEPES, 0.2 MgATP, 7 $MgCl_2$, 1 $CaCl_2$, 10 EGTA, and 5–20 μM GTPγS (290 mmol/kg; pH 7.2). In this solution the free Ca^{2+} concentration was kept at ~35 nM. In some experiments secretion was stimulated by a combination of GTP and high free Ca^{2+}. In these cases the pipette contained (in mM) 125 K-glutamate, 10 HEPES, 0.2 MgATP, 7 $MgCl_2$, 9.2 $CaCl_2$, 10 EGTA, and 1.6 GTP (290 mmol/kg; pH 7.2), for a calculated free Ca^{2+} concentration of 900 nM.

The chromaffin cell and CHO cell pipette solution contained (mM) 120 Cs-glutamate, 20 HEPES, 5 MgATP, 5 $MgCl_2$, 1 $CaCl_2$, and 10 EGTA (290 mmol/kg; pH 7.2).

Cell inflation

To inflate a patch-clamped cell, we applied pressure to the interior of the patch pipette with a water manometer. Pressures in the range of 1–30 cm H_2O could be applied with this system.

Measurements of exocytosis

We used two different techniques to monitor exocytosis in inflated cells: measurements of the cell membrane capacitance to follow the fusion of individual secretory granules, and amperometry to follow the release of serotonin from individual fusion events.

The cell membrane capacitance was measured with a software phase-sensitive detector as described before (Joshi and Fernandez, 1988; Fidler and Fernandez, 1989). The phase detector was implemented with a personal computer (P5-66; Gateway 2000), a data acquisition interface board (AT-MIO-16X; National Instruments), and an EPC-7 patch-clamp amplifier (List Electronics, Darmstadt, Germany). The software phase detector was written in LabView (National Instruments). Recordings were made in the whole-cell mode of the patch-clamp technique. The command voltage applied to a patch-clamped cell was composed of the sum of a sinusoidal voltage (833 Hz, 54 mV peak to peak, filtered at 830 Hz) and a holding potential (typically 0 mV). The membrane current was measured at two phase angles, $I_{\varphi+0}$, $I_{\varphi+90}$, relative to the stimulus. The phase angle φ was chosen with the phase tracking technique (Fidler and Fernandez, 1989). The phase angle was adjusted periodically so that the output at $I_{\varphi+0}$ reflected changes in the real part of the cell admittance ($Re[\Delta Y]$), whereas the output at $I_{\varphi+90}$ reflected changes in the imaginary part of the cell admittance ($Im[\Delta Y]$), which is proportional to changes in the cell membrane capacitance.

In some cases we recorded vesicle fusion and serotonin release simultaneously. The release of serotonin was measured by the amperometric technique as described before (Kawagoe et al., 1991; Wightman et al., 1991). A sealed glass electrode made from an 8-μm carbon fiber was connected to an EPC-7 patch-clamp amplifier and held at 650 mV. The redox current was low pass filtered at Nyquist and sampled by the same data acquisition board as used in the capacitance measurements.

Scanning electron microscopy

The medium was removed by aspiration, and the cells were washed three times with phosphate-buffered saline (PBS) (pH 7.2). Cells were fixed with 4% paraformaldehyde–1% glutaraldehyde in PBS, for 10 min at room temperature. Then cells were rinsed in PBS three times and then dehydrated in a graded series of ethanol (i.e., 60%, 70%, 80%, 95%, 100% 2×, 15 min each). The glass coverslips, reimmersed in 100% ethanol, were dried in a critical point drier (Ted Pella, Redding, CA). The resulting coverslips were mounted on aluminum studs and coated with a ~150-Å layer of gold and palladium in a 60:40 ratio, by using a Danton 502A vacuum evaporator. Cells were examined with a Jeol 6400 scanning electron microscope. Micrographs were taken with a Polaroid type 55 positive/negative film.

RESULTS

Inflation of mast cells reversibly blocks exocytosis

Patch-clamped cells can be inflated by applying a finely calibrated pressure to the interior of the patch pipette. Mast cells patch clamped in the whole-cell recording mode can be inflated by an average of 3.8 ± 1.6 (n = 26) times their original volume by applying a pressure of 5–15 cm H_2O to the interior of the patch pipette. A typical experiment is shown in Fig. 1. Within 15 s after the whole-cell configuration was established, a pressure of 9 cm of H_2O was applied to the patch pipette (Fig. 1 *A*). Mast cells typically inflate slowly, beginning within 2 min after the pipette pressure is increased. The extent of inflation depends on the applied pressure until a limit is reached. At this point, the diameter of the inflated cell does not increase when the pressure is elevated further. This is the point of maximum inflation (Fig. 1 *B*). If the pressure is increased beyond this range, the cell bursts. A mast cell can be kept inflated for long periods of time. An inflated cell has a striking mor-

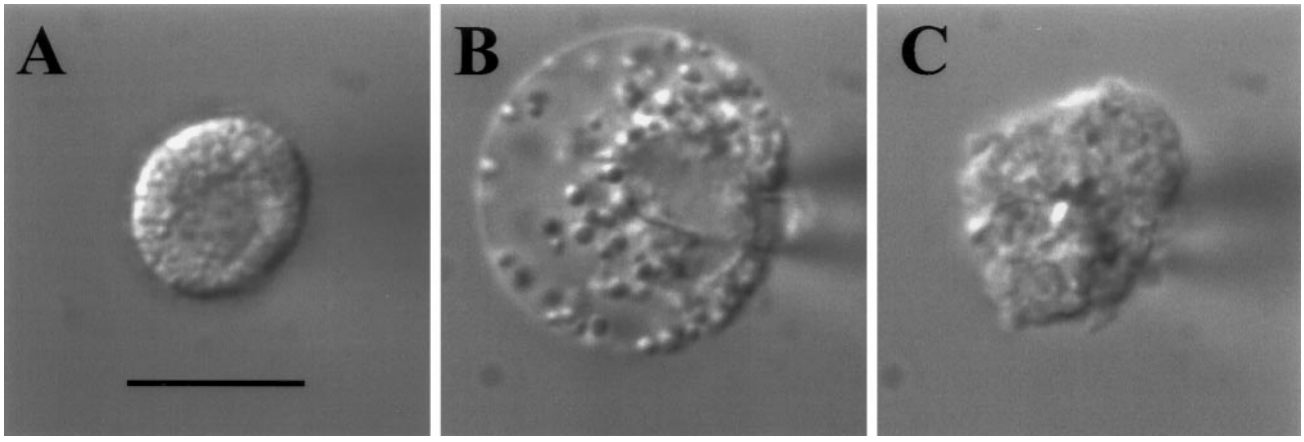

FIGURE 1 Inflation of a mast cell delays degranulation and thoroughly perfuses the cell's cytosol. (*A*) A mast cell patch-clamped in the whole-cell recording mode. The cell was perfused with a pipette solution containing GTPγS (5 μM) to trigger exocytotic degranulation. (*B*) Before degranulation began, the cell was inflated by applying 10 cm H_2O to the interior of the patch pipette. The mast cell could remain inflated up to 1 h without degranulating. (*C*) As the pipette pressure returned to 0 cm H_2O, the cell slowly regained its original size and then completely degranulated in a normal fashion. The picture shows the cell after full degranulation.

phological appearance. In an inflated mast cell the cytosolic volume can increase by up to sevenfold (see Fig. 3 *C*), and the secretory granules become separated from each other; however, they do not undergo Brownian motion and appear to be fixed, as if attached to stretched cytoskeletal structures. A small group of granules remained docked to the plasma membrane of the inflated cell (Fig. 1 *B*).

In our experiments we included GTPγS in the pipette solutions to trigger a secretory response. It is critical that a cell begin to inflate before any secretory activity begins. We have observed that if we delayed the application of pipette pressure and allowed the cell to begin degranulating, pressures of up to 30 cm H_2O failed to inflate the cells and arrest the degranulation. However, if a cell begun inflating before degranulation, pressures in the range of 3–20 cm H_2O were sufficient to reach maximum inflation. In an inflated cell, degranulation did not occur (Fig. 1 *B*). Upon removal of the pipette pressure, we observed the mast cells return, slowly, to their normal size, as if the cell were an elastic structure that could be reversibly stretched. After the cells returned to their original size, they degranulated fully (Fig. 1 *C*).

To examine the secretory activity of a mast cell during and after inflation, we monitored the cell membrane capacitance (Fig. 2). A mast cell perfused with 5 μM GTPγS begins to degranulate within 5 min after the onset of perfusion. The degranulation is recorded as a long staircase of step increases in the cell membrane capacitance (Fig. 2 *A*). Each step corresponds to the fusion of a single secretory granule. A degranulation comprises several hundred steps, which are observed over a period of time.

If a cell is inflated before exocytosis begins, the large increases in cell membrane capacitance that result from degranulation are not seen for as long as the cell remains inflated (Fig. 2 *B*). Removal of the pipette pressure allows the cell to recover its original size and then degranulate. This delayed degranulation is recorded as a large number of step increases in capacitance that occur with a high frequency 1.65 ± 0.77 events/s (data from 16 cells; 0.5–10 μM GTPγS; Fig. 2 *B*). However, during inflation we do observe a small number of fusion events that occur at a much lower frequency, 0.025 ± 0.034 events/s (data from 27 cells). Hence the frequency of fusion is reduced by ~66 times by inflation of a cell. Experiments done at higher concentrations of GTPγS (200–400 μM) give a similar result where the frequency of fusion events in inflated cells was low, 0.037 ± 0.021 events/s (nine cells), and during degranulation after deflation was high, 2.93 ± 1.17 events/s (four cells).

The experiments shown in Fig. 2, *A* and *B*, demonstrate that the secretory machinery remains intact in inflated cells and that upon deflation, the molecular structures responsible for granule fusion reassemble and become functional again. Interestingly, the reassembly of the molecular scaffold regulating fusion can be completely blocked by perfusing the cell's cytosol with solutions containing pronase (1 mg/ml). In cells inflated with solutions containing pronase, we observed a steady decrease in the cell membrane capacitance, without the step increases that are characteristic of fusion events. We never observed a degranulation upon deflation of these cells (Fig. 2 *C*).

Recent patch-clamp studies of exocytosis in mast cells have shown that degranulation triggered by GTPγS can be blocked by an excess of GTP (Oberhauser et al., 1992). Similar studies showed that degranulation could also be triggered by pipette solutions containing GTP and an elevated free calcium concentration (Fernandez et al., 1984). These observations suggested that GTP and Ca^{2+}-binding proteins form part of the trigger mechanism that activates granule fusion during exocytosis. We have observed similar responses in cells that have been inflated for prolonged periods of time and then allowed to degranulate. A summary of these observations is shown in Table 1.

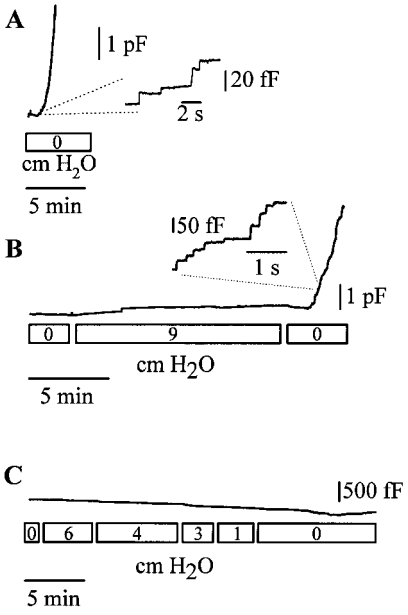

FIGURE 2 Capacitance measurements of exocytotic degranulation in inflated cells. (*A*) Measurement of the cell membrane capacitance of a mast cell undergoing degranulation in response to perfusion with 5 μM GTPγS. The open bar beneath the recording indicates the time of application and pressure applied to the patch pipette. This cell was not inflated and responded within 60 s of the beginning of whole-cell recording. As shown by the inset, the large increase in the cell membrane capacitance is composed of steps, marking the fusion of individual secretory granules. (*B*) Capacitance recordings in a patch-clamped mast cell, similar to *A*, but inflated by a pressure of 9 cm H_2O. The cell was kept inflated for ~15 min. During inflation only a small increase in capacitance is seen. Within 2 min after the pressure returned to 0 cm H_2O, the cell degranulated and the capacitance increased in a stepwise fashion. (*C*) A patch-clamped mast cell inflated by a pressure of 6 cm H_2O. Degranulation was completely blocked by including pronase (1 mg/ml) in the pipette solution. In all cases, degranulation was triggered by including 5 μM GTPγS in the pipette solutions.

Recently it was demonstrated that an *N*-ethyl-maleimide (NEM)-sensitive protein called *N*-ethylmaleimide sensitive factor (NSF) played a major role in the regulation of intracellular traffic (Malhotra et al., 1988; Rothman and Orci, 1992). Furthermore, NSF was found to associate with synaptic vesicle proteins, and thus it was proposed that NSF and several other proteins formed a "fusion machine" that regulated both constitutive and regulated vesicular fusion (Söllner et al., 1993; Söllner, 1995; Südhof, 1995). In view of these developments, we predicted that degranulation of inflated mast cells would be sensitive to reducing agents like NEM. We inflated mast cells with our standard pipette solutions, to which we added 5 μM GTPγS to trigger degranulation. We attempted to block the degranulation of these mast cells by adding various reducing agents to the pipette solutions. We added 0.5–1 mM NEM ($n = 5$); 0.1–1 mM dithiothreitol ($n = 7$); 1.4 mM mercaptoethanol ($n = 3$), and 5 mM L-cysteine ($n = 3$). We kept the cells inflated for 30–60 min with these pipette solutions; however, in all cases, the cells promptly degranulated upon deflation.

The specific membrane capacitance of inflated cells

The specific membrane capacitance of mammalian cells is thought to be close to 1 μF/cm^2 (Hille, 1992). The specific cell membrane capacitance, C_m, of inflated and resting cells was calculated as the ratio between the total membrane capacitance C_T and the surface area of the plasma membrane. The cell membrane area was calculated from the cell diameter, measured from video images of the patch-clamped cells. The total cell membrane capacitance, C_T, was measured by using the compensation circuitry of the EPC-7 patch clamp. As Table 2 shows, C_m is calculated to be 1.02 $\pm$ 0.29 μF/cm^2 in resting mast cells and 0.50 $\pm$ 0.06 μF/cm^2 (12 cells) in maximally inflated cells. Note that C_T changed very little with inflation (from 4.00 $\pm$ 1.41 to 4.30 $\pm$ 1.79 pF; see also Fig. 2 *B*). The computation of the specific cell membrane capacitance relies on an accurate measurement of the cell membrane surface area. The apparent differences between the initial and inflated values of C_m are likely to be the result of errors in the estimation of the cell membrane surface area. In particular, cells typically have a large number of surface specializations that are too small to be seen with a regular optical microscope. To examine the surface topography of mast cells, we fixed and processed them for scanning electron microscopy (Fig. 3, *A* and *B*). Fig. 3 *A* shows an electron micrograph of a typical mast cell with a large number of plasma membrane expansions and folds. Although we cannot rule out the possibility that some of the surface membrane features resulted from fixation artifacts, such surface membrane specializations have been shown to be typical of peritoneal mast cells (e.g.,

TABLE 1 Exocytotic responses observed in mast cells after inflation

Pipette solution	Inflation pressure (cm H_2O)	$C_T^{initial}$ (pF)	$C_T^{response}$ (pF)
GTPγS (5 μM)	11 $\pm$ 4 (n=14)	5.25 $\pm$ 0.66	12.13 $\pm$ 0.85 (14:0)
GTP + Ca^{2+} (1.6 mM; 900 nM)	13 $\pm$ 8 (n= 6)	5.81 $\pm$ 0.49	9.55 $\pm$ 0.26 (5:1)
GTPγS + GTP (5 μM; 2 mM)	10 $\pm$ 5 (n= 6)	5.45 $\pm$ 1.72	5.45 $\pm$ 2.15 (1:5)
GTPγS + Pronase (5 μM; 1 mg/ml)	12 $\pm$ 5 (n= 5)	4.25 $\pm$ 1.00	2.45 $\pm$ 1.29 (0:5)

The table lists the observed membrane capacitance changes in mast cells dialyzed with different solutions and inflated to their maximum size. The initial cell membrane capacitance, $C_T^{initial}$ (pF), was measured soon after the establishment of the whole-cell mode. Afterward, the cells were inflated for a period of time ranging between 15 min and 1 h. Several minutes after the pipette pressure was reduced to 0 cm H_2O, we measured the magnitude of the exocytotic response by measuring the cell membrane capacitance, $C_T^{response}$ (pF). The number of cells tested is indicated by (n) in the second column. The number of cells that degranulated after recovery from inflation and the number of cells that did not degranulate after inflation are indicated as (d:nd) in the last column.

TABLE 2 The specific cell membrane capacitance and apparent diameter of inflated cells

Cell type	$C_T^{initial}$ (pF)	$d^{initial}$ (μm)	$C_m^{initial}$ (μF/cm^2)	$C_T^{inflated}$ (pF)	$d^{inflated}$ (μm)	$C_m^{inflated}$ (μF/cm^2)
Mast (n = 12)	4.00 ± 1.41	11.12 ± 0.85	1.02 ± 0.29	4.30 ± 1.79	16.20 ± 2.82	0.50 ± 0.06
Chromaffin (n = 12)	5.82 ± 1.62	15.40 ± 0.26	0.78 ± 0.20	6.23 ± 1.83	19.14 ± 2.54	0.53 ± 0.04
CHO (n = 3)	7.02 ± 2.78	14.82 ± 2.22	0.99 ± 0.09	7.60 ± 2.26	21.15 ± 2.48	0.53 ± 0.03

The specific cell membrane capacitance of inflated cells is 0.5 μF/cm^2. The measurements were made in three different cell types: mast cells (n = 12), chromaffin cells (n = 12), and CHO cells (n = 3). All cells were inflated to their maximum size before bursting. The table shows the specific cell membrane capacitance $C_m^{initial}$ (μF/cm^2) calculated, before inflation, from the values of the total cell membrane capacitance $C_T^{initial}$ (pF) and the apparent diameter of the cell $d^{initial}$ (μm). Similarly, we calculated the specific cell membrane capacitance during maximum inflation $C_m^{inflated}$ (μF/cm^2), which is shown to be 0.5 μF/cm^2 in all three cell types.

Hide et al., 1993; Fawcett, 1981) and of mammalian cells in general (Fawcett, 1981). The majority of these surface specializations are invisible to the optical microscope, introducing an error in the determination of the cell membrane surface area. Maximum inflation of a cell by means of a patch pipette is likely to smooth out these structures. Thus a cell membrane surface area calculated from the diameter of an inflated cell would be more accurate. These considerations suggest that the true specific cell membrane capacitance of a mast cell is ~0.5 μF/cm^2. We measured the effect of inflation on the calculated specific capacitance of two other cell types, chromaffin cells and CHO cells, and found results similar to those of mast cells (Table 2). Chromaffin cells had an initial total cell capacitance, C_T, of 5.82 ± 1.62 pF, which increased slightly to 6.2 ± 1.83 pF after inflation. The calculated initial specific membrane capacitance was 0.78 ± 0.2 μF/cm^2 and dropped to 0.53 ± 0.04 μF/cm^2 upon inflation (n = 12; Table 2). Similarly, CHO cells had an initial total capacitance, C_T, of 7.02 ± 2.78 pF, which also increased slightly to 7.6 ± 2.26 pF upon inflation. The calculated initial specific capacitance was 0.99 ± 0.09 μF/cm^2 and dropped to 0.53 ± 0.03 μF/cm^2 upon inflation (n = 3; Table 2). It is striking that very different cell types converge to the same specific membrane capacitance when the surface membrane area is calculated from inflated cells. These results suggest that the specific cell membrane capacitance of mammalian cells is close to 0.5 μF/cm^2, rather than the widely accepted value of 1 μF/cm^2.

Our observations suggest that cell inflation is carried out at a constant surface membrane area, where the increase in cell volume is made possible by smoothing out the surface

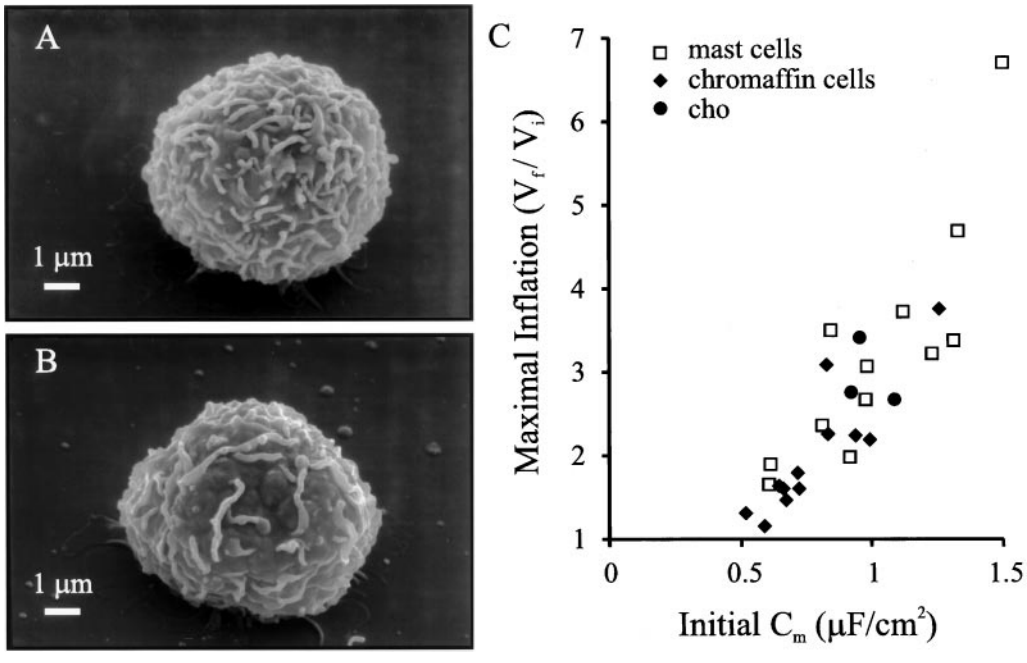

FIGURE 3 The extent to which a cell can be inflated depends on the folds of its surface membrane. The degree of folding varies greatly from cell to cell. (*A*) Scanning electron micrograph of a mast cell rich in plasma membrane folds. Inflation of the cell would flatten the folds, allowing the cell to expand. (*B*) Another mast cell with fewer membrane folds. (*C*) The specific cell membrane capacitance of a cell, measured at rest, is a good predictor of the maximum increase in the size of a cell observed upon inflation. Inflation is expressed as the ratio between the estimated final and initial volumes of the cell, V_f/V_i. The extent of inflation is linearly related to the initial specific capacitance. A value of specific membrane capacitance larger than 0.5 μF/cm^2 indicates the presence of surface folds that will allow the cell to expand. The figure shows data from mast cells (n = 12), chromaffin cells (n = 12), and CHO cells (n = 3).

structures that are typical of a mammalian cell. Furthermore, we have found that the specific cell membrane capacitance is 0.5 μF/cm^2. Hence we predict that a resting cell that has a calculated specific membrane capacitance close to 0.5 μF/cm^2 will not have many surface structures and will not increase in size significantly upon inflation. By contrast, a resting cell with a calculated specific capacitance larger than 0.5 μF/cm^2 has a large number of surface structures and will expand more upon inflation. Indeed, this is demonstrated in the graph of Fig. 3 *C*. As the figure shows, those cells that have a calculated specific capacitance larger than 0.5 μF/cm^2 can be inflated more. This graph confirms the view that the true value of the cell membrane capacitance is 0.5 μF/cm^2 and suggests that there is a great deal of variability in the number of membrane specializations, from cell to cell. This variability is evident when the scanning micrographs of two different mast cells are compared (Fig. 3, *A* and *B*).

During the inflation of mast cells, if the cell expands at constant area, we do not expect any changes in the total cell membrane capacitance. The small increase in total cell capacitance observed upon inflation remains unexplained. We examined this small increase in total cell capacitance with high-resolution capacitance recordings of the type shown in Fig. 2. We found that an increase in the pipette pressure always caused a slow and smooth increase in membrane capacitance (Fig. 4 *B*), which was fully reversible (Fig. 4 *A*), and its amplitude depended on the size of the pressure jump (36 $\pm$ 5 fF/cm H_2O; $n = 10$). It is likely that in mast cells, fusion events that occur during inflation will also contribute to the small increase in capacitance observed. However, because this increase is less than 10% of the total cell capacitance, it introduces only a small error into the estimate of the specific capacitance of the cell membrane.

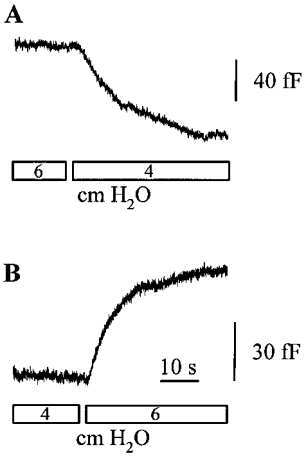

FIGURE 4 Inflation or deflation causes small, smooth, and reversible changes in the cell membrane capacitance. (*A*) Membrane capacitance recording of an inflated mast cell experiencing a decrease in pressure from 6 to 4 cm H_2O. (*B*) In the same cell, the membrane capacitance increases upon returning to the higher pressure value. These changes were fully reversible, were typically smaller than 100 fF, and were observed in all inflated cells.

Anomalous capacitance steps in inflated cells

Although exocytosis is inhibited in inflated cells (see Fig. 2 *B*), high-resolution capacitance recordings can follow in detail the few fusion events that do occur. Fig. 5 shows typical experiments. A fusion event measured in a cell inflated with 5 cm H_2O appears as a simple step increase in the capacitance of the cell membrane. Upon an increase in the pressure to 8 cm H_2O, there is a smooth increase in capacitance, similar to those demonstrated in Fig. 4. However, fusion events no longer appeared as simple capacitance steps. Upon the fusion of a single granule, a rapid rise in capacitance is followed, after a variable time, by a drop that then recovers to complete the step (Fig. 5 *A*). This pattern is also evident in a cell inflated with 11 cm H_2O. However, in this case the size of the drop in capacitance is bigger.

Fig. 6 shows an analysis of the patterns observed in the capacitance recordings of single granule fusion events recorded in maximally inflated cells. The inset of Fig. 6 *A*

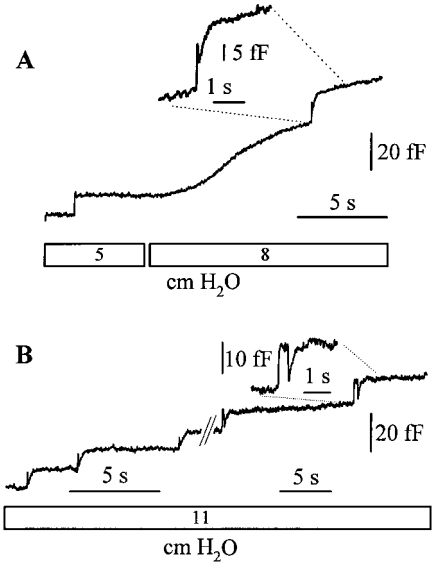

FIGURE 5 Inflation modifies the kinetics of fusion of single granules with the plasma membrane. (*A*) Membrane capacitance recording during progressive inflation of a mast cell. As in Fig. 4, the membrane capacitance slowly increased after the pressure inside the patch pipette was changed from 5 to 8 cm H_2O. The figure shows two granules that fused with the plasma membrane and increased the cell membrane capacitance in a stepwise manner. The fusion event recorded at 5 cm H_2O caused a simple step increase in the cell membrane capacitance as it is commonly observed. However, at 8 cm H_2O, the fusion event causes a capacitance increase that follows a complex time course. This is better illustrated in *B*, where several fusion events were recorded at 11 cm H_2O. The figure shows that a fusion event causes a transient increase in capacitance, which then increases exponentially to its final value. This complex time course is only observed upon inflation of a cell. If the pressure is removed, fusion events cause stepwise increases in the cell membrane capacitance, as observed in Fig. 2 *B*.

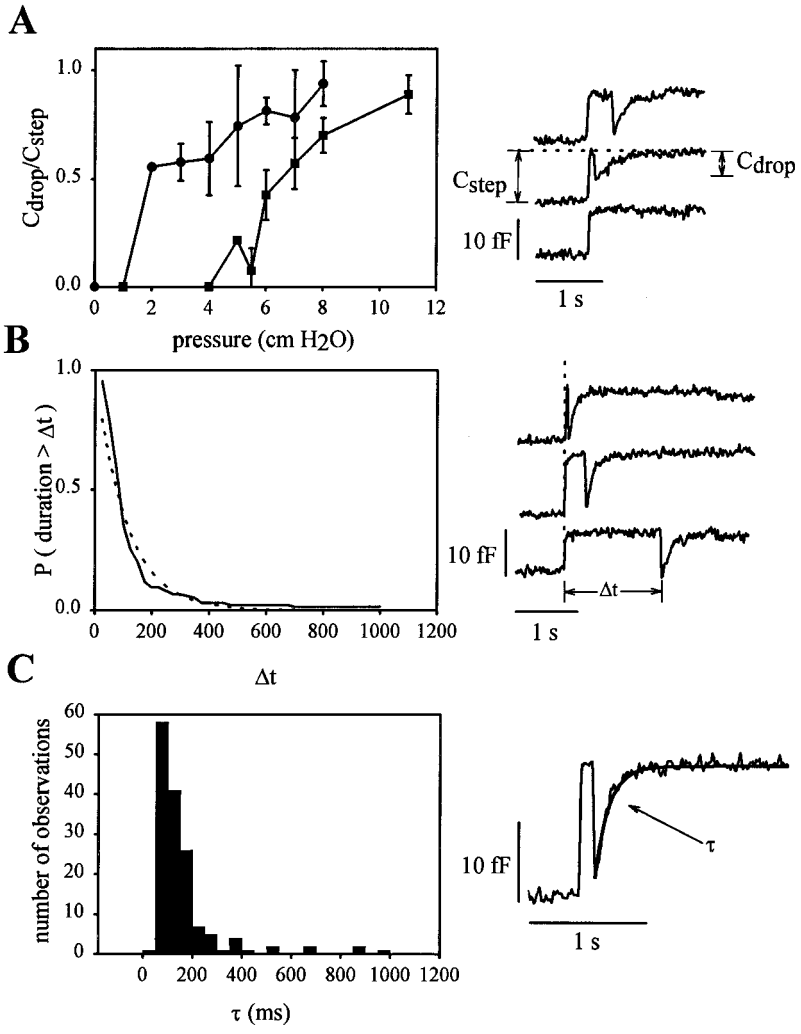

FIGURE 6 Pressure dependency and kinetics of single granule fusion events during inflation. (*A*) The complex kinetics of single fusion events recorded during inflation is pressure dependent. As the inset shows, capacitance recordings of fusion events under pressure are marked by an initial stepwise increase, C_{step}, which then abruptly drops and recovers exponentially to its initial value. The size of the capacitance drop (C_{drop}) is pressure dependent and is represented by the ratio C_{drop}/C_{step}. In the graph, the curves refer to two different cells. (*B*) The duration of the transient phase, measured as Δt (see *inset*), has a probability distribution (*thick line*) that is well represented by an exponential function with a time constant of 105 ms (*dashed line*). (*C*) The recovery after the drop in capacitance is exponential (see *thick line in inset*). A histogram of the measured time constants reveals that the majority of the values occur between 50 and 200 ms.

shows that the size of the drop in capacitance is dependent on the applied pressure. As the inset shows, a reduction in pressure from 11 cm H_2O to 7 cm H_2O and then to 1 cm H_2O (*top to bottom*) causes a reduction in the size of the capacitance drop, until it is no longer noticeable. The graph of Fig. 6 *A* summarizes this finding. The figure shows the size of the capacitance drop, normalized by the final size of the capacitance step, as a function of the applied pressure. Recordings from two different cells are shown. The data show that there is a threshold pressure at which the drop appears. In the case of the first cell, this threshold is 2 cm H_2O. The threshold for the other cell is 5 cm H_2O. In both cells, the ratio of C_{drop}/C_{step} saturates at higher pressures at a value close to 1, indicating that the size of the drop is equal to the size of the capacitance step.

The capacitance recordings shown in the inset of Fig. 6 *B* show that the time between the first indication of fusion (a step rise in the capacitance) and the appearance of the capacitance drop, Δt, varies over a wide range. The graph of Fig. 6 *B* shows the probability distribution function for Δt. We fitted the distribution with an exponential function, which gave a best fit with a time constant of 105 ms (Fig. 6 *B, dotted line in the graph*). The average value for Δt was 126 ms ($n = 134$), which is close to the value of the exponential fit.

The recovery from the drop in capacitance is exponential. The inset of Fig. 6 *C* shows a large drop in the capacitance, recorded from an inflated mast cell at a pressure of 8 cm H_2O. The recovery phase was fitted with an exponential. The time constant of the best fit was 121 ms. The graph in Fig. 6 *C* shows a histogram of the time constant values obtained from 134 events similar to that shown in the inset. The average value of the exponential fits was 148 ms ($n = 134$).

The phase-sensitive detection of changes in the admittance of a secretory cell gives two simultaneous outputs: $I_{\varphi+0}$ and $I_{\varphi+90}$. The capacitance trace corresponds to $I_{\varphi+90}$ and measures the imaginary part of the changes in the admittance of the cell (Joshi and Fernandez, 1988). $I_{\varphi+0}$ measures the real part of the admittance changes and is proportional to changes in the input conductance of the cell. Fig. 7 shows both outputs, $I_{\varphi+0}$ and $I_{\varphi+90}$, recorded during fusion events in a maximally inflated cell. As the figure shows, the drop in the capacitance recording is sometimes

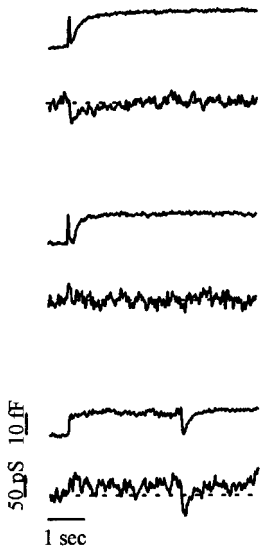

FIGURE 7 Sometimes the capacitance drop that marks fusion events under pressure is paralleled by a drop in the input conductance of the cell. The figure shows four recordings of the changes in the input conductance caused by fusion events in an inflated mast cell. The capacitance recordings (*top traces*) show drops of various magnitudes, which may or may not be paralleled by a drop in the input conductance of the cell (*bottom traces*).

paralleled by a significant decrease in $I_{\varphi+0}$. However, this pattern was not always observed. Sometimes the capacitance drop occurred without a measurable change in $I_{\varphi+0}$.

Capacitance recordings of the type demonstrated here are a sensitive assay of exocytotic fusion. It has been shown that the opening and closure of the fusion pore can be observed as changes in the cell membrane capacitance. Thus it is easy to conclude that the drop in capacitance, observed in inflated cells, corresponds to the transient closure of the fusion pore. However, the simple experiment of Fig. 8 proves that this view is wrong. Fig. 8 shows simultaneous capacitance and amperometric recordings of fusion events

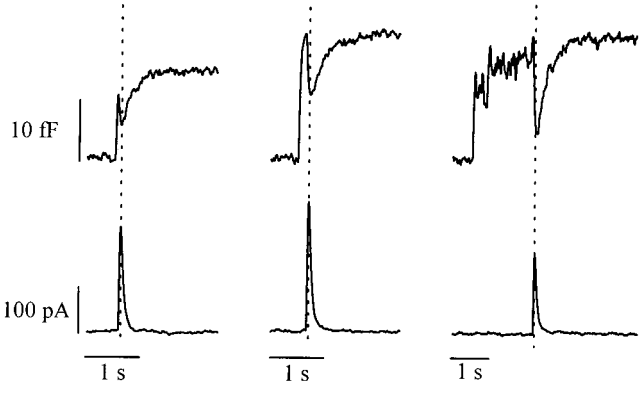

FIGURE 8 Simultaneous capacitance and amperometric recordings of single exocytotic events in an inflated mast cell. An amperometric spike marks the release of the bulk of the serotonin upon exocytosis of a single secretory granule. The serotonin spike always occurs during the drop in capacitance that characterizes the fusion events measured in inflated mast cells.

measured in maximally inflated cells at a pressure of 9–10 cm H_2O. The capacitance trace shows the characteristic drop. Surprisingly, the amperometric spike that marks the release of serotonin always occurs at exactly the time that the drop begins. This observation is significant because it is now understood that the amperometric spike corresponds to the time of maximum enlargement of the fusion pore (Alvarez de Toledo et al., 1993; Marszalek et al., 1996). Hence the experiment shown in Fig. 8 suggests than the drop in capacitance is not due to closure of the fusion pore; rather, it occurs precisely when the fusion pore becomes largest and the bulk of the serotonin is released.

Transient fusion events in inflated cells

A transient fusion event is characterized by a step increase in the cell membrane capacitance, followed after some time by a step decrease in the capacitance. This pattern was interpreted as an indication that a fusion pore formed transiently (Fernandez et al., 1984; Spruce et al., 1990; Oberhauser and Fernandez, 1996). A striking feature of the transient fusion events observed in mast cells is that the size of the off capacitance step is always slightly bigger than the size of the on step (Monck et al., 1990; Oberhauser and Fernandez, 1996). This difference, ΔC_T, was dependent on the open dwell time of the fusion pore and had a magnitude of $\Delta C_T \approx 1.6$ fF/s. These results suggested that during the time that the fusion pore remained open, there was a flux of lipids, from the plasma membrane into the granule membrane, at a rate of $\sim 10^6$ lipids/s. This observation was interpreted as an indication that the membrane of the secretory granule was under tension, causing a net flux of lipids from the plasma membrane, through the fusion pore and into the granule membrane.

In contrast to resting mast cells, transient fusion events recorded in maximally inflated mast cells have similar on and off capacitance step sizes (Fig. 9). A fit of the data showed that $\Delta C_T = -0.01$ fF/s. A long transient fusion event was excluded from the figure. This event lasted 21.6 s and showed a $\Delta C_T = -4$ fF. If this event is included in the fit, then the slope becomes -0.16 fF/s. Hence, in inflated cells, ΔC_T is between -0.01 and -0.16 fF/s. This value is reversed and is much smaller than that of the transient fusion events observed in mast cells that are not inflated (1.4–1.7 fF/s; Monck et al., 1990; Oberhauser and Fernandez, 1996).

DISCUSSION

Inflation of mast cells

Mast cells contain several hundred secretory granules, which are tightly packed in the cytosol. Upon inflation, most secretory granules became separated from each other and from the plasma membrane. However, a small number of granules remained attached to the plasma membrane as if they were docked. Surprisingly, the cytosolic granules did

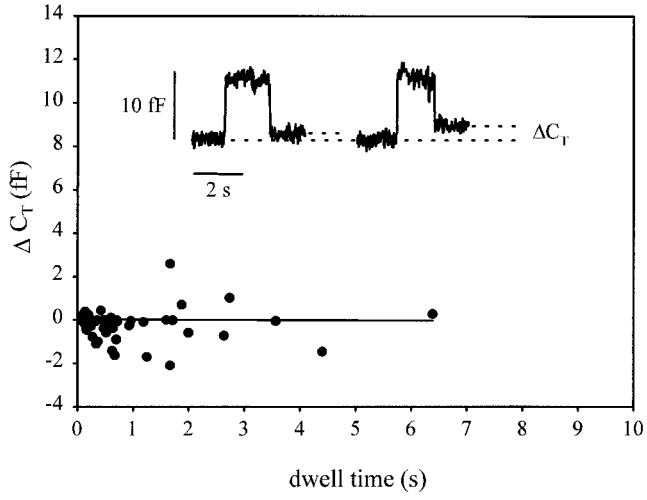

FIGURE 9 An analysis of transient fusion events in inflated cells reveals that the size of the off step, ΔC_{off}, is equal to or slightly smaller than that of the on step, ΔC_{on}. The difference, $\Delta C_T = \Delta C_{off} - \Delta C_{on}$, is typically either zero or negative. The inset shows two examples of transient fusion events in maximally inflated mast cells. The graph shows the value of ΔC_T versus the dwell time of the transient fusion event ($n = 62$). A fit of the data (*thick line*) gives a slope of -0.01 fF/s.

not undergo Brownian motion, indicating that they were firmly attached to cytoskeletal structures that were stretched but remained intact throughout inflation. Upon removal of the pipette pressure, inflated cells regained their original size without further intervention. This observation suggests that the elastic components that held the secretory granules span the cell diameter and are capable of retracting the cell membrane when the pressure is removed. It is interesting to note that we could not inflate cells that had started to secrete. This was true for mast cells and for chromaffin cells. This observation suggests that the elastic modulus of these unknown cytoskeletal strings increased during secretion. These findings are in agreement with the observation that secretory cells stiffen during secretion (Liu et al., 1987).

The role of soluble proteins in mast cell secretion

Inflation of a patch-clamped cell, by means of a manometer, provides us with a certain way to perfuse a cell, overcoming the difficulties associated with a purely diffusional exchange between the patch pipette and the cell. By using the cell inflation technique described here, high-molecular-weight substances can be introduced into the cytosol of cells without having to wait for diffusional exchange. Furthermore, during inflation soluble cytosolic proteins will move from the cytosol into the pipette. An inflated mast cell (radius 8 μm) has a volume of 2.1 pl, which is negligible compared with the volume of the pipette solution, which is $\sim$15 μl. An inflated cell with a final diameter of 15 μm and a pipette access resistance of 8 MΩ will exchange 99% of a large protein (MW 110,000) within 20 min (Pusch and Neher, 1988; Okano et al., 1993). Smaller proteins will exchange faster. Thus it is reasonable to expect that a cell inflated for 30–60 min will have diluted all soluble components of the cytosol by more than a million-fold. This level of dilution is equivalent to complete inactivation. Surprisingly, we have observed that mast cells inflated for long periods of time promptly degranulate upon deflation, indicating that the reassembly and activation of the fusion pore scaffold do not require soluble proteins.

However, several soluble cytosolic proteins have been proposed to play key roles in cellular membrane fusion. Among these are NSF and α-soluble NSF attachment protein, both of which have been shown to be required for Golgi transport. We have tested the effect of NEM in mast cells. Cells were inflated with pipette solutions containing 1 mM NEM in addition to the standard 5 μM GTPγS used to trigger exocytosis. Cells have remained inflated with NEM for periods as long as 40 min; however, in all cases the cells degranulated completely upon deflation. We have also tested the effect of other reducing agents that open disulfide bonds like dithiothreitol, mercaptoethanol, and cysteine. None of these agents prevented the full exocytotic degranulation of inflated cells. These results are surprising in view of the central role proposed for NSF on exocytotic secretion. However, Morgan and Burgoyne (1995) have recently showed evidence suggesting that NSF and soluble NSF attachment protein may function as molecular chaperones that enable vesicle docking, but do not have a direct role in fusion.

The membrane tension of inflated cells

An important advantage of cell inflation with patch pipettes is that it allows for a fine control of the tension in the cell membrane. A mast cell can be inflated near its breaking point by applying a pipette pressure of 10–15 cm H_2O. At this point the cell becomes large, has a spherical appearance, and is said to be maximally inflated. A mast cell maximally inflated with pressures of $\sim$11 cm H_2O typically reaches a diameter of $\sim$16 μm (Tables 1 and 2). A pressure (P) of 11 cm H_2O corresponds to 1.1×10^3 N/m^2. According to Laplace's law, the tension (T) in the membrane of a thin-walled sphere of diameter d is given by $T = Pd/4$. Hence a mast cell maximally inflated with 11 cm H_2O and a final diameter of 16 μm will develop a plasma membrane tension $T = 4.4$ mN/m. Although lysis of inflated cells was not investigated (in fact it was avoided), maximally inflated cells typically lysed if the pressure was increased further. Hence mast cell lysis probably occurs in the range of 5–8 mN/m. This range is similar to that observed in yeast (6–11 mN/m; Gustin et al., 1988) and red blood cells (6–12 mN/m; Evans et al., 1976), but higher than that in pure lipid vesicles (3–4 mN/m; Kwok and Evans, 1981).

Exocytosis is inhibited by 60-fold in maximally inflated mast cells (see Results). This inhibition must result, in part, from the mechanical separation of the secretory granules that occurs during inflation (see Fig. 1 *B*). However, it is

likely that a membrane tension of 4.4 mN/m is also a cause of the inhibition. In the scaffold model of exocytosis, the fusion pore is formed by first dimpling the plasma membrane into a sharp tip that then fuses spontaneously with the granule membrane (Monck and Fernandez, 1994). Indeed, electron microscopy studies have shown that the first step in an exocytotic response is the dimpling of the plasma membrane of secretory cells (Chandler and Heuser, 1980; Ornberg and Reese, 1981). Dimpling of the plasma membrane is likely to be resisted by a membrane tension of 4.4 mN/m, causing inhibition in the early stages of formation of the fusion pore.

Our data support the view that the loss of plasma membrane observed during transient fusion events, ΔC_T, corresponds to a tension-driven flux of lipid molecules through the exocytotic fusion pore (Monck et al., 1990). The putative flux of lipids through the fusion pore observed during transient fusion events is calculated from a $\Delta C_T \approx 1.6$ fF/s to be 10^6 lipid molecules/s (Monck et al., 1990). Because ΔC_T was reversed by inflation to a value of -0.01 fF/s, we calculate a flux of $\sim -10^4$ lipid molecules/s (Fig. 9). Although not measured directly, a granule membrane tension of 0.1 mN/m is sufficient to explain a flux of 10^6 plasma membrane lipid molecules/s, through a 2-nm-wide fusion pore and into the granule membrane (Nanavati et al., 1992). An increase in the plasma membrane tension from $\sim$0.1–0.001 mN/m (at rest) to 4.4 mN/m would reverse the direction of the lipid flow, as observed. If this view is correct, it is surprising that given the large reversal in membrane tension, a larger outward flux of lipids is not observed. However, whereas the resting plasma membrane represents a large pool of lipids that are free to move, the granule membrane fits tightly onto the gel matrix of the granule and therefore is unlikely to be capable of a sustained loss. Hence, although tension may reverse the flow of lipids through the fusion pore, the granule membrane cannot be the source of a continuous stream of lipids, limiting the outward flux or perhaps arresting it.

Under tension, individual fusion events show a characteristic drop in capacitance that is coincidental with the release of the bulk of the granular serotonin. Thus the latency observed between the initial increase in capacitance and the drop in capacitance is identical to the latency between the onset of fusion and the bulk release of serotonin. This latency has been explained as the time it takes for the fusion pore to expand (Alvarez de Toledo et al., 1993; Monck et al., 1991). Furthermore, this latency was shown to depend on the size of the vesicles and the intracellular free calcium concentration (Alvarez de Toledo et al., 1993; Fernández-Chacón and Alvarez de Toledo, 1995). In mast cells of the beige mouse, the average value of the latency between the onset of fusion and bulk serotonin release is $\sim$370 ms (Alvarez de Toledo et al., 1993). This value coincides with the average length of time required for fusion pore expansion ($\sim$400 ms; Monck et al., 1991). The probability distribution function of the latencies can be fitted by an exponential with a time constant of $\sim$200 ms (Monck et al., 1991). The discrepancy between the values of the time constant and the average may have been the result of nonexponential terms in the distribution caused by the wide range of sizes of the giant beige granules (with an average diameter of 2.6 μm).

Wild-type mast cells have smaller granules (average diameter of 0.7 μm) and faster latencies. In inflated mouse mast cells, the latency between the onset of fusion and the capacitance drop is well described by an exponential distribution function with a time constant of 105 ms, which is close to its average of 126 ms (Fig. 6 *B*). This latency falls within the range of latencies measured for rat mast cells (58–230 ms; Alvarez de Toledo et al., 1993; Fernández-Chacón and Alvarez de Toledo, 1995), suggesting that a plasma membrane tension of $\sim$4 mN/m does not significantly change the length of time required for the expansion of the fusion pore.

The membrane capacitance of inflated cells

In the absence of evidence other than microscopic images, the large increase in the diameter of a cell observed upon inflation (e.g., Fig. 1) could have at least three sources: an increase in the cell membrane area that occurs at constant membrane volume and causes membrane thinning, a large expansion of the surface membrane area caused by exocytosis, and finally, smoothing out of surface projections that are invisible to the optical microscope. If the total cell membrane capacitance did not change at all during cell inflation, it would be possible to rule out any contribution from membrane thinning and from exocytosis, and we would readily conclude that the expansion of the cell diameter is due entirely to the smoothing out of the surface of the cell membrane. However, during inflation we always observe that the cell membrane capacitance does increase slightly. Thus it is likely that all three factors contribute, in different degrees, to the increase in the size of the cell upon inflation.

Membrane thinning causes only small effects. For example, a pipette pressure of 1 cm H_2O applied to the interior of a spherical cell ($d = 16$ μm) causes an isotropic membrane tension, T, of 0.4 mN/m. The area elastic modulus of a red blood cell membrane, K, has been found to be 450 mN/m (Evans et al., 1976). The fractional change in membrane area, $\Delta\alpha = \Delta A/A_0$, is given by $\Delta\alpha = T/K$. Hence $\Delta\alpha = 8.9 \times 10^{-4}$/cm H_2O, or a 0.089% increase in surface membrane area for every cm H_2O of applied pressure. Because the cell membrane expands at constant volume, the membrane thins, also increasing the specific capacitance by 0.089%/cm H_2O. Then we calculate that a mast cell with $C_T = 4$ pF would increase its total capacitance by $\sim$7 fF/cm H_2O because of membrane expansion and thinning. This value is smaller than the 36 fF/cm H_2O that is actually observed (see Results). A mast cell maximally inflated to a diameter of 16 μm with a pipette pressure of 11 cm H_2O will develop a membrane tension of 4.4 mN/m, which will

expand the cell membrane by only 0.98%, causing an increase in the total cell membrane capacitance of ~77 fF and a 0.98% increase in the specific cell membrane capacitance due to thinning. However, expansion and thinning estimates based on the area elastic modulus of red blood cells must be viewed with caution. For example, in a careful study of the mechanical properties of patches of chick skeletal muscle membrane, Sokabe et al. (1991) found an area elastic modulus of ~50 mN/m. Hence the area elastic modulus of mast cells probably lies between 50 and 500 mN/m and may fully explain the small increases in capacitance observed upon inflation. Regardless of its extent, tension-driven membrane expansion must remain less than the 2–3% that is known to cause cell lysis (Needham and Hochmuth, 1989) and will always be a small part of the ~200% increase in the calculated surface membrane area of an inflated cell.

In inflated mast cells the frequency of fusion events is reduced 66 times. However, we always observed a few fusion events. The total number of fusion events depended on the length of time that the cell remained inflated. For example, if a mast cell remained maximally inflated for 30 min with pipette solutions containing 5 mM GTPγS, we expect to observe a total of only ~45 fusion events. A typical step increase in capacitance is 15 fF. Hence we expect an increase of total cell membrane capacitance of only 675 fF or an increase of ~17% in the surface area of the inflated cell.

These observations suggest that only small increases in the cell membrane area will result from membrane thinning and from exocytosis. The main cause of the large increase in the diameter of the cell is likely to be the smoothing out of the large number of surface structures that are typically observed in their surface (Fig. 3, *A* and *B*). This view is supported by the finding that the degree of inflation of a given cell can be predicted from the calculated specific cell membrane capacitance at rest (Fig. 3 *C*). We conclude that most of the inflation of a cell occurs at constant surface membrane area.

It is generally accepted that the specific capacitance of cellular membranes is 1 μF/cm^2 (e.g., Hille, 1992); however, values up to 3 μF/cm^2 have been reported in hepatocytes (Graf et al., 1995), indicating that most of the cell membrane is folded by numerous microvilli and canaliculi. When a biological membrane is stretched out, the measured specific capacitance is lower (e.g., 0.7 μF/cm^2; Sokabe et al., 1991). Indeed, our results show that the specific membrane capacitance of inflated cells is 0.5 μF/cm^2. It is likely that the diameter of an inflated cell is a true reflection of its total surface membrane and therefore allows for an accurate measurement of surface membrane area. The remarkable agreement in the value of the specific capacitance of the three inflated cell types supports the view that the cell membrane of mammalian cells has a specific capacitance of 0.5 μF/cm^2. This result is only half of the universally accepted value of 1 μF/cm^2; however, it is in the range of the specific membrane capacitance of artificial lipid bilayers (e.g., White, 1977).

Capacitance recordings of a fusion event in an inflated cell

Exocytotic fusion events recorded from inflated mast cells have a striking appearance. Upon fusion, a step increase in capacitance is rapidly followed by a drop that recovers exponentially (e.g., Fig. 6). This observation has so far defied a quantitative explanation. Our data show that the drop in the capacitance recording occurs at precisely the time when the bulk of the serotonin is released (Fig. 8). These results suggest that the drop in capacitance occurs only when the fusion pore is large. This is surprising, because it cannot be explained by our current view of the electrical events that follow an exocytotic fusion event. The electrical equivalent circuit of a fusing secretory vesicle is modeled as a capacitance (the granule membrane) in series with a resistor (the fusion pore). Admittance measurements can detect exocytotic fusion events by monitoring the real ($Re[\Delta Y]$) and imaginary ($Im[\Delta Y]$) components of the change in cell admittance caused by the fusion of a secretory vesicle (Breckenridge and Almers, 1987; Zimmerberg et al., 1987; see also Experimental Procedures). What is normally called a "capacitance recording" corresponds to the imaginary part of the changes in cell admittance ($Im[\Delta Y]$). According to the fusion model, $Im[\Delta Y]$ equals the vesicular membrane capacitance only when the fusion pore is large. At this time the value of $Im[\Delta Y]$ reaches its maximum and the bulk of the stored secretory products are released (e.g., Alvarez de Toledo et al., 1993). In sharp contrast, exocytotic events recorded in inflated cells show a pressure-dependent drop in $Im[\Delta Y]$ at precisely the time when the fusion pore is largest and bulk release occurs. These observations strongly suggest that the series capacitor and resistor equivalent circuit with which we typically describe a fusion event is incomplete.

Recent work has shown that mast cell secretory granules are filled with a densely charged and cross-linked ion exchange gel (Curran and Brodwick, 1991; Fernandez et al., 1991; Marszalek et al., 1996). The mast cell gels were shown to have surprising electrical and mechanical properties (Nanavati and Fernandez, 1993; Parpura and Fernandez, 1996) and to behave as semiconductive junctions when placed in an asymmetrical electric field (Marszalek et al., 1995a,b). The ion exchange gels have not been considered in the electrical equivalent circuits used to model vesicular fusion. However, it is likely that the electrical properties of these gels play a role in the changes in $Im[\Delta Y]$ observed upon fusion. If this view is correct, the effect of the electrical properties of the gels becomes apparent in inflated cells, and only when the fusion pore is large. The drop in $Im[\Delta Y]$ could be explained if we assumed that the gel, which is electrically in series with the fusion pore, becomes a poor conductor while releasing the bulk of serotonin by an ion exchange mechanism. It is also possible that the fusion pore becomes literally "plugged" by the pressure-driven exudation of the granule matrix.

It is also interesting to consider that during transient fusion events, we have observed that the size of the off capacitance step is always slightly bigger that the size of the on step (Monck et al., 1990; Oberhauser and Fernandez, 1996). We have speculated that this is due to flow of lipids through the fusion pore, driven by a tension gradient, where the tension of the granule membrane is higher than that of the plasma membrane (Monck et al., 1990). It is significant that the anomalous capacitance steps (see Fig. 6) occur under conditions where the tension of the plasma membrane is increased and the putative flow of lipids through the fusion pore would be either arrested or reversed (see Fig. 9). It is possible that these phenomena play a complex and yet unknown role in the electrical properties of the fusion pore. From these considerations it is evident that a more detailed understanding of the electrical events associated with vesicle fusion will be necessary to model an adequate equivalent circuit for vesicular fusion events and to fully explain our observations.

REFERENCES

Alvarez de Toledo, G., R. Fernandez-Chacón, and J. M. Fernandez. 1993. Release of secretory products during transient vesicle fusion. *Nature.* 363:554–558.

Breckenridge, L. J., and W. Almers. 1987. Currents through the fusion pore that forms during exocytosis of a secretory vesicle. *Nature.* 328: 814–817.

Chandler, D. E., and J. E. Heuser. 1980. Arrest of membrane fusion events in mast cells by quick-freezing. *J. Cell Biol.* 86:666–674.

Curran, M. J., and M. S. Brodwick. 1991. Ionic control of the size of the vesicle matrix of beige mouse mast cells. *J. Gen. Physiol.* 98:771–790.

Dai, J., and M. P. Sheetz. 1995. Mechanical properties of neuronal growth cone membranes studied by tether formation with laser optical tweezers. *Biophys. J.* 68:988–996.

Du, X. Y., and S. Sorota. 1997. Cardiac swelling-induced chloride current depolarizes canine atrial myocytes. *Am. J. Physiol.* 272(4 Pt 2): H1904–H1916.

Evans, E. A., R. Waugh, and L. Melnik. 1976. Elastic area compressibility modulus of red cell membrane. *Biophys. J.* 16:585–595.

Fawcett, D. W. 1981. The Cell. W.B. Saunders Co., Philadelphia, PA 19105.

Fernandez, J. M., E. Neher, and B. D. Gomperts. 1984. Capacitance measurements reveal stepwise fusion events in degranulating mast cells. *Nature.* 312:453–455.

Fernandez, J. M., M. Villalón, and P. Verdugo. 1991. Reversible condensation of mast cell secretory products in vitro. *Biophys. J.* 59:1022–1027.

Fernández-Chacón, R., and G. Alvarez de Toledo. 1995. Cytosolic calcium facilitates release of secretory products after exocytotic vesicle fusion. *FEBS Lett.* 363:221–225.

Fidler, N., and J. M. Fernandez. 1989. Phase tracking: an improved phase detection technique for cell membrane capacitance measurements. *Biophys. J.* 56:1153–1162.

Graf, J., M. Rupnik, G. Zupancic, and R. Zorec. 1995. Osmotic swelling of hepatocytes increases membrane conductance but not membrane capacitance. *Biophys. J.* 68:1359–1363.

Gustin, M., X. L. Zhou, B. Martinac, and C. Kung. 1988. A mechanosensitive ion channel in the yeast plasma membrane. *Science.* 242:762–765.

Hide, I., J. P. Bennett, A. Pizzey, G. Boonen, D. Bar-Sagi, B. D. Gomperts, and P. E. Tatham. 1993. Degranulation of individual mast cells in response to Ca^{2+} and guanine nucleotides: an all-or-none event. *J. Cell Biol.* 123:585–593.

Hille, B. 1992. Ionic Channels in Excitable Membranes. Sinauer Associates, Sunderland, MA. 9–11.

Hochmuth, F. M., J. Y. Shao, J. Dai, and M. P. Sheetz. 1996. Deformation and flow of membrane into tethers extracted from neuronal growth cones. *Biophys. J.* 70:358–369.

Joshi, C., and J. M. Fernandez. 1988. Capacitance measurements. An analysis of the phase detector technique used to study exocytosis and endocytosis. *Biophys. J.* 53:885–892.

Kawagoe, K. T., J. A. Jankowski, and R. M. Wightman. 1991. Etched carbon fiber electrodes as amperometric detectors of catecholamine secretion from isolated biological cells. *Anal. Chem.* 63:1589–1594.

Kemble, G. W., T. Danieli, and J. M. White. 1994. Lipid-anchored influenza hemagglutinin promotes hemifusion, not complete fusion. *Cell.* 76:383–91.

Kwok, R., and E. A. Evans. 1981. Thermoelasticity of large lecithin bilayer vesicles. *Biophys. J.* 35:637–652.

Liu, Z. Y., J. I. Young, and E. L. Elson. 1987. Rat basophilic leukemia cells stiffen when they secrete. *J. Cell Biol.* 105:2933–2943.

Malhotra, V., L. Orci, B. S. Glick, M. R. Block, and J. E. Rothman. 1988. Role of an *N*-ethylmaleimide-sensitive transport component in promoting fusion of transport vesicles with cisternae of the Golgi stack. *Cell.* 54:221–227.

Marszalek, P. M., B. Farrell, and J. M. Fernandez. 1996. Ion-exchange gel regulates neurotransmitter release through the exocytotic fusion pore. *Soc. Gen. Physiol. Ser.* 51:211–222.

Marszalek, P. M., V. S. Markin, T. Tanaka, H. Kawaguchi, and J. M. Fernandez. 1995a. The secretory granule matrix-electrolyte interface: a homologue of the p-n rectifying junction. *Biophys. J.* 69:1218–1229.

Marszalek, P. M., V. S. Markin, T. Tanaka, H. Kawaguchi, and J. M. Fernandez. 1995b. Pulsed laser imaging demonstrates the mechanism of current rectification at a hydrogel interface. *Langmuir.* 11:4196–4198.

Matsuda, N., N. Hagiwara, M. Shoda, H. Kasanuki, and S. Hosoda. 1996. Enhancement of the L-type Ca^{2+} current by mechanical stimulation in single rabbit cardiac myocytes. *Circ. Res.* 78:650–659.

Monck, J. R., G. Alvarez de Toledo, J. M. Fernandez. 1990. Tension in secretory granule membranes causes extensive membrane transfer trough the exocytotic fusion pore. *Proc. Natl. Acad. Sci. USA.* 87: 7804–7808.

Monck, J. R., and J. M. Fernandez. 1994. The exocytotic fusion pore and neurotransmitter release. *Neuron.* 12:707–716.

Monck, J. R., A. F. Oberhauser, G. Alvarez de Toledo, and J. M. Fernandez. 1991. Is swelling of the secretory granule matrix the force that dilates the exocytotic fusion pore? *Biophys. J.* 59:39–47.

Morgan, A., and R. D. Burgoyne. 1995. Is NSF a fusion protein? *Trends Cell Biol.* 5:335–339.

Nanavati, C., and J. M. Fernandez. 1993. The secretory granule matrix: a fast acting smart polymer. *Science.* 259:963–965.

Nanavati, C., V. S. Markin, A. F. Oberhauser, and J. M. Fernandez. 1992. The exocytotic fusion pore modeled as a lipidic pore. *Biophys. J.* 63:1118–1132.

Needham, D., and R. M. Hochmuth. 1989. Electro-mechanical permeabilization of lipid vesicles. Role of membrane tension and compressibility. *Biophys. J.* 55:1001–1009.

Oberhauser, A. F., and J. M. Fernandez. 1996. Hydrophobic ions amplify the capacitative currents used to measure exocytotic fusion. *Biophys. J.* 69:451–459.

Oberhauser, A. F., J. R. Monck, W. E. Balch, and J. M. Fernandez. 1992. Exocytotic fusion is activated by Rab3a peptides. *Nature.* 360:270–273.

Okano, K., J. R. Monck, and J. M. Fernandez. 1993. GTPγS stimulates exocytosis in patch-clamped rat melanotrophs. *Neuron.* 11:165–172.

Ornberg, R. L., and T. S. Reese. 1981. Beginning of exocytosis captured by rapid-freezing of *Limulus* amebocytes. *J. Cell. Biol.* 90:40–54.

Parpura, V., and J. M. Fernandez. 1996. Atomic force microscopy study of the secretory granule lumen. *Biophys. J.* 71:2356–2366.

Pusch, M., and E. Neher. 1988. Rates of diffusional exchange between small cells and a measuring patch pipette. *Pflügers Arch.* 411:204–211.

Rothman, J. E., and L. Orci. 1992. Molecular dissection of the secretory pathway. *Nature.* 355:409–415.

Setoguchi, M., Y. Ohya, I. Abe, and M. Fujishima. 1997. Stretch-activated whole-cell currents in smooth muscle cells from mesenteric resistance artery of guinea-pig. *J. Physiol. (Lond.).* 501(Pt 2):343–353.

Sokabe, M., F. Sachs, and Z. Jing. 1991. Quantitative video microscopy of patch clamped membranes stress, strain, capacitance, and stretch channel activation. *Biophys. J.* 59:722–728.

Söllner, T. 1995. SNAREs and targeted membrane fusion. *FEBS Lett.* 369:80–83.

Söllner, T., S. W. Whiteheart, M. Brunner, H. Erdjument-Bromage, S. Geromanos, P. Tempst, and J. E. Rothman. 1993. SNAP receptors implicated in the vesicle targeting and fusion. *Nature.* 362:318–324.

Spruce, A. E., L. J. Breckenridge, A. K. Lee, and W. Almers. 1990. Properties of the fusion pore that forms during exocytosis of the mast cell secretory vesicle. *Neuron.* 4:643–654.

Südhof, T. C. 1995. The synaptic vesicle cycle: a cascade of protein-protein interactions. *Nature.* 375:645–653.

White, S. H. 1977. Studies of the physical chemistry of planar bilayer membranes using high-precision measurements of specific capacitance. *Ann. N.Y. Acad. Sci.* 303:243–265.

Wightman, R. M., J. A. Jankowski, R. T. Kennedy, K. T. Kawagoe, T. J. Schroeder, D. J. Leszcyszyn, J. A. Nera, E. J. Diliberto, Jr., and O. H. Viveros. 1991. Temporally resolved catecholamine spikes correspond to single vesicle release from individual chromaffin cells. *Proc. Natl. Acad. Sci. USA.* 88:10754–10758.

Zimmerberg, J., M. Curran, F. S. Cohen, and M. Brodwick. 1987. Simultaneous electrical and optical measurements show that membrane fusion precedes secretory granule swelling during exocytosis of beige mouse mast cells. *Proc. Natl. Acad. Sci. USA.* 84:1585–1589.

Zimmerberg, J., S. S. Vogel, and L. V. Chernomordik. 1993. Mechanisms of membrane fusion. *Annu. Rev. Biophys. Biomol. Struct.* 22:433–466.